

# Basin-scale distribution patterns of photosynthetic picoeukaryotes along an Atlantic Meridional Transect

Amy R. Kirkham,<sup>1</sup> Ludwig E. Jardillier,<sup>1†</sup>  
Ana Tiganeşcu,<sup>1</sup> John Pearman,<sup>1</sup> Mikhail V. Zubkov<sup>2</sup>  
and David J. Scanlan<sup>1\*</sup>

<sup>1</sup>Department of Biological Sciences, University of Warwick, Coventry, UK.

<sup>2</sup>National Oceanography Centre, Southampton, Hampshire SO14 3ZH, UK.

## Summary

Photosynthetic picoeukaryotes (PPEs) of a size < 3 µm play a crucial role in oceanic primary production. However, little is known of the structure of the PPE community over large spatial scales. Here, we investigated the distribution of various PPE classes along an Atlantic Meridional Transect sampled in boreal autumn 2004 that encompasses a range of ocean provinces (gyres, upwelling, temperate regions), using dot blot hybridization technology targeting plastid 16S rRNA gene amplicons. Two algal classes, Prymnesiophyceae and Chrysophyceae, dominated the PPE community throughout the Atlantic Ocean, over a range of water masses presenting different trophic profiles. However, these classes showed strongly complementary distributions with Chrysophyceae dominating northern temperate waters, the southern gyre and equatorial regions, while prymnesiophytes dominated the northern gyre. Phylogenetic analyses using both plastid and nuclear rRNA genes revealed a high diversity among members of both classes, including sequences contained in lineages with no close cultured counterpart. Other PPE classes were less prevalent along the transect, with members of the Cryptophyceae, Pelagophyceae and Eustigmatophyceae essentially restricted to specific regions. Multivariate statistical analyses revealed strong relationships between the distribution patterns of some of these latter PPE classes and temperature, light intensity and nutrient concentrations. Cryptophyceae, for example, were

mostly found in the upwelling region and associated with higher nutrient concentrations. However, the key classes of Prymnesiophyceae and Chrysophyceae were not strongly influenced by the variables measured. Although there appeared to be a positive relationship between Chrysophyceae distribution and light intensity, the complementary distributions of these classes could not be explained by the variables recorded and this requires further explanation.

## Introduction

Approximately half of the global CO<sub>2</sub> fixation occurs in marine systems (Field *et al.*, 1998), with the vast spatial areas occupied by open ocean regions predicted to be responsible for a large majority of this primary production (Pauly and Christensen, 1995). Organisms ≤ 3 µm in size are the major players in marine CO<sub>2</sub> fixation and, while such photosynthetic picoplankton are dominated numerically by the prokaryotic genera *Prochlorococcus* and *Synechococcus*, much of the fixed carbon is attributable to the eukaryotic fraction (Li, 1994; Marañón *et al.*, 2001; Worden *et al.*, 2004; Jardillier *et al.*, 2010). Phylogenetic analyses of the eukaryotic fraction performed using both nuclear (18S rRNA) and plastid (16S rRNA) molecular markers have revealed a large diversity among these photosynthetic picoeukaryotes (PPEs) (Díez *et al.*, 2001; Moon-van der Staay *et al.*, 2001; Vaultot *et al.*, 2002; 2008; Massana *et al.*, 2004; Yuan *et al.*, 2004; Fuller *et al.*, 2006a; Lovejoy *et al.*, 2006; Worden, 2006; Not *et al.*, 2007a,b; Worden and Not, 2008), with members of all known algal classes detected. Other molecular tools, such as whole-cell analyses using fluorescent *in situ* hybridization (FISH) (Not *et al.*, 2002; 2008), and DNA dot blot hybridization techniques (Fuller *et al.*, 2006b; McDonald *et al.*, 2007; Lepère *et al.*, 2009), have begun to provide further insight into PPE community structure and dynamics. However, there is still a relative dearth of information on the distribution of the dominant PPE classes over large spatial scales (though see Liu *et al.*, 2009). This is crucial to identifying the major players involved in marine CO<sub>2</sub> fixation and the biotic and abiotic factors controlling their abundance.

The Atlantic Meridional Transect (AMT) project capitalizes on the passage of the British Antarctic Survey vessel from the UK, allowing measurements and samples to be

Received 19 May, 2010; accepted 20 November, 2010. \*For correspondence. E-mail d.j.scanlan@warwick.ac.uk; Tel. (+44) 24 76 528363; Fax (+44) 24 76 523701. †Present address: Unité d'Ecologie, Systématique et Evolution, UMR CNRS 8079 Univ. Paris-Sud, 91405 Orsay, France.

taken regularly over a large extent of the Atlantic Ocean (Aiken and Bale, 2000). The programme began in 1995 and has completed 19 transects up until November 2009. Each AMT cruise is sequentially numbered, with AMT1 being the first cruise in 1995 (Robinson *et al.*, 2006). The AMT extends between the UK and either the Falkland Islands, Cape Town in South Africa or southern Chile. It crosses four major circulation features of the Atlantic Ocean observed by Hooker and colleagues (2000): the North Atlantic Gyre (NAG), 50–25°N; the Tropics and Equatorial Region (TER) 25°N–15°S; the South Atlantic Gyre (SAG), 15–35°S; and the Sub-Antarctic Convergence Zone (SACZ) south of 35°S. Several provinces (Longhurst, 2007) further dissect the transect between mesotrophic temperate and coastal regions, oligotrophic gyres and upwelling regions. Thus, the Atlantic Ocean is characterized by strong nutrient and temperature gradients, which could influence the distribution pattern of major PPE groups.

Previous pigment analyses along AMT cruises have shown values for total chlorophyll *a* (Tchl<sub>a</sub>) inferred biomass to be highest in the northern and southern temperate zones and in the Benguela or north-west African upwelling regions with > 1 mg m<sup>-3</sup> Tchl<sub>a</sub> (Gibb *et al.*, 2000; Aiken *et al.*, 2009). In contrast, the tropical and subtropical regions have the lowest Tchl<sub>a</sub> concentrations (< 0.25 mg m<sup>-3</sup>). These latter regions, largely encompassing the oligotrophic gyres, are dominated by *Prochlorococcus*, as assessed both by flow cytometry (Zubkov *et al.*, 2000) and pigments (Gibb *et al.*, 2000; Aiken *et al.*, 2009). On the other hand, PPEs are observed in much lower numbers, but because of their larger size contribute significantly to total phytoplankton biomass. For instance, in equatorial waters of AMT3 PPEs formed a pronounced deep maximum with concentrations up to 10 000 cells ml<sup>-1</sup>, corresponding to 15 mg C m<sup>-3</sup>, contrasting with a local surface maximum of *Synechococcus* off the Mauritanian upwelling of 100 000 cells ml<sup>-1</sup>, equating to just 20 mg C m<sup>-3</sup> (Zubkov *et al.*, 1998). PPEs are present at all latitudes, tending to show highest concentrations in temperate waters at either end of the transect and at depths of 40–80 m in the equatorial section (Zubkov *et al.*, 2000), distribution patterns similar to those of *Synechococcus* (Zubkov *et al.*, 1998). More specific analyses of photosynthetic carotenoids and accessory pigments show fucoxanthin and peridinin (suggestive of diatoms, dinoflagellates and prymnesiophytes) and alloxanthin (indicative of cryptophytes) to be found at maximum concentrations in temperate and upwelling regions while 19'-hexanoyloxyfucoxanthin, 19'-butanoyloxyfucoxanthin and chlorophyll *b* (suggestive of prymnesiophytes, chrysophytes and chlorophytes, respectively), have broader distribution patterns but again are higher in temperate and upwelling regions (Gibb *et al.*, 2000). While such pigment

distributions are more or less indicative of specific taxa, problems still arise when attempting to define the composition of specific phytoplankton size classes (Aiken *et al.*, 2009).

To address this latter issue, and to resolve PPE distribution patterns over the basin scale and a range of ocean provinces, we applied dot blot hybridization analysis using class-specific oligonucleotide probes along an AMT cruise undertaken in boreal autumn 2004 (AMT15). Moreover, plastid and nuclear rRNA gene clone libraries were constructed to reveal the extent of phylogenetic diversity among the classes detected. Using a range of ancillary data collected on the same cruise, we also began to resolve the biotic and abiotic factors that might explain the distribution patterns of specific taxa.

## Results

### *Chemical and physical characteristics of AMT15*

AMT15 extended from 48°N (south-west of the UK) to 40°S (SW of Cape Town, South Africa) (Fig. 1). Temperate regions (48–39°N and 31–40°S) were characterized by nutrient concentrations that ranged between 0.019 and 0.09 μM NO<sub>2</sub>, 0.03–8.2 μM NO<sub>3</sub> and 0.17–0.62 μM PO<sub>4</sub>, while much lower values were found in the northern (38–

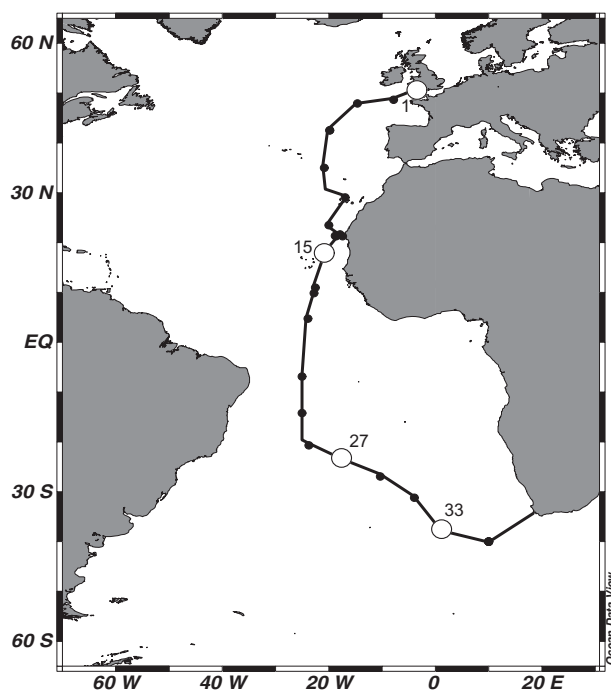


**Fig. 1.** AMT15 cruise track. Closed circles indicate the position of stations for which samples were used for dot blot hybridization analysis at six depths corresponding to surface, 55%, 33%, 14%, 1% and 0.1% of surface light intensity. Clone libraries were constructed at stations 1, 15, 27 and 33, and are marked with large open circles.

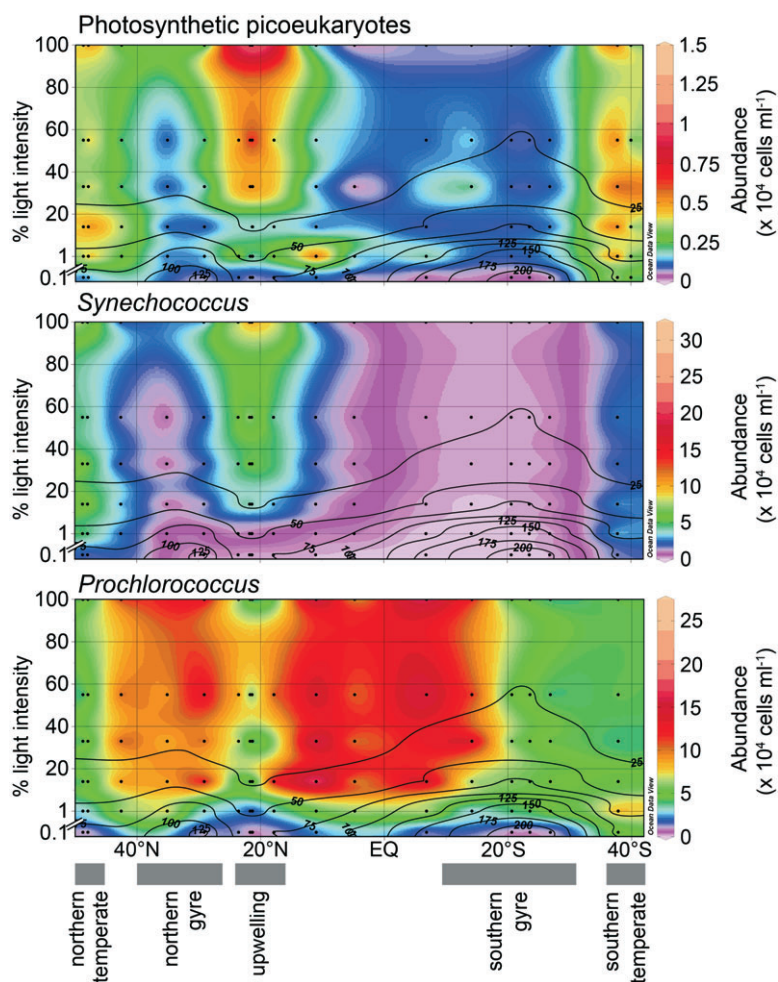


**Fig. 2.** Photosynthetic picoplankton distribution patterns along AMT15. Assessment of the abundance (cells  $\text{ml}^{-1}$ ) of PPEs (top), *Synechococcus* (middle) and *Prochlorococcus* (bottom) as determined by flow cytometry. Data for these latter two groups has been previously reported (see Zwirgmaier *et al.*, 2007). For each panel the y-axis is the light intensity (% surface irradiance) and the x-axis latitude (degrees north or south of the equator). Black contour lines indicate the depth in metres, black dots represent sampling points. Note the break in the y-axis.

30°N) and southern (6–30°S) gyre (0.0005–0.02  $\mu\text{M}$   $\text{NO}_2$ , 0.01–0.03  $\mu\text{M}$   $\text{NO}_3$  and 0.002–0.02  $\mu\text{M}$   $\text{PO}_4$ ), though up to 0.7  $\mu\text{M}$   $\text{PO}_4$  was recorded in the southern gyre below 15°S. In contrast, the west African upwelling region (21°N) possessed the highest nutrient concentrations measured along the transect (0.003–0.71  $\mu\text{M}$   $\text{NO}_2$ , 0.01–26.2  $\mu\text{M}$   $\text{NO}_3$  and 0.02–1.53  $\mu\text{M}$   $\text{PO}_4$ ). Surface temperatures were 16–19°C in the northern temperate region and 12–13°C in the southern temperate region, 22–28°C in the gyres and 21–23°C in the upwelling area (see Zwirgmaier *et al.*, 2007 and Fig. S1 for more details).

#### Photosynthetic picoplankton abundance along AMT15

The peak abundance of PPEs, as revealed by flow cytometry (Fig. 2), occurred towards the northern (48°N) and southern (40°S) extremes of the transect, reaching  $1 \times 10^4$  cells  $\text{ml}^{-1}$  and  $8.5 \times 10^3$  cells  $\text{ml}^{-1}$  respectively. The upwelling area also had a peak in abundance of  $1.3 \times 10^4$  cells  $\text{ml}^{-1}$ . Less than  $3.4 \times 10^3$  cells  $\text{ml}^{-1}$  were found along the eastern edge of the northern gyre, and in the southern gyre abundance remained below 900 cells  $\text{ml}^{-1}$ . This dis-

tribution pattern appears to be similar to that reported for *Synechococcus* (Zwirgmaier *et al.*, 2007), which had peaks of  $1 \times 10^5$ ,  $3.6 \times 10^4$  and up to  $3 \times 10^5$  cells  $\text{ml}^{-1}$  in the northern and southern temperate and upwelling regions, respectively, and in contrast to *Prochlorococcus*, which peaked in the gyres and equatorial region with up to  $1.5 \times 10^5$  and  $2 \times 10^5$  cells  $\text{ml}^{-1}$  respectively (Zwirgmaier *et al.*, 2007).

#### Distribution patterns of PPE classes

Of the 10 class-specific probes used in dot blot hybridization analysis, seven reached values above 2%. These were the probes detecting the classes Prymnesiophyceae, Chrysophyceae, Cryptophyceae, Pelagophyceae, Pinguicophyceae, Trebouxiophyceae and Eustigmatophyceae (Fig. 3). The sum of relative hybridization values for all probes averaged 40% across all stations and depths, but ranged from as low as 4% relative hybridization at the 0.1% light level in the southern gyre (stations 21 and 25) up to 100% at the 55% light level in the Northern temperate region (station 3). The most

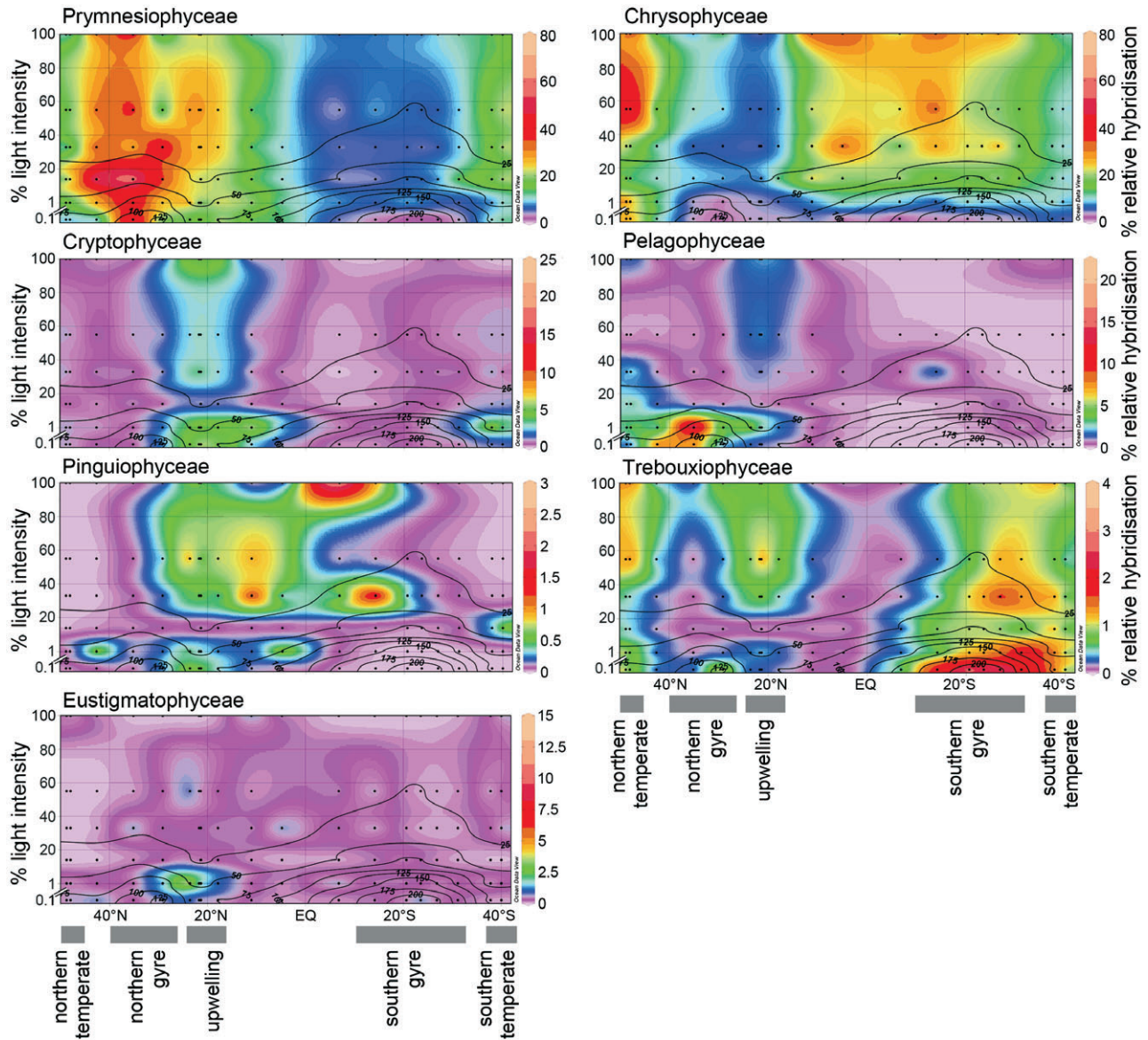


**Fig. 3.** Dot blot hybridization data showing the distribution of specific PPE classes along the AMT15 transect. Contour plots indicate the % relative hybridization (as a proportion of all amplified by primers PLA491F and OXY1313R). *x*- and *y*-axes are as described in Fig. 2. Black contour lines indicate the depth in metres, black dots represent sampling points.

abundant classes over the transect were the Pymnesiophyceae and the Chrysophyceae, both of which had maximum values of 70% relative hybridization. These two major classes showed a strikingly complementary distribution (Fig. 3). Pymnesiophyceae had highest relative hybridization values in the northern gyre and lowest values in the southern gyre whereas Chrysophyceae had highest values in the northern temperate region and in the southern gyre, and very low values in the northern gyre.

The relative hybridization values for the other classes were considerably lower. Cryptophyceae reached a peak abundance of 23% relative hybridization, at 0.1% light intensity, at an upwelling station around 20°N. However,

for the rest of the transect relative hybridization values for the Cryptophyceae remained below 10%. Pelagophyceae reached 22% relative hybridization at one northern gyre station at a depth corresponding to 1% light intensity, but was below the background level for much of the transect except in the northern gyre and upwelling regions. Pinguiphyceae, Trebouxiophyceae and Eustigmatophyceae reached peak relative hybridization values of 3%, 4% and 15% respectively (Fig. 3).

Canonical correspondence analysis (CCA) showed that measured environmental variables could explain up to 48% of the variation in dot blot hybridization data i.e. in PPE class proportions. The 10 key variables associated

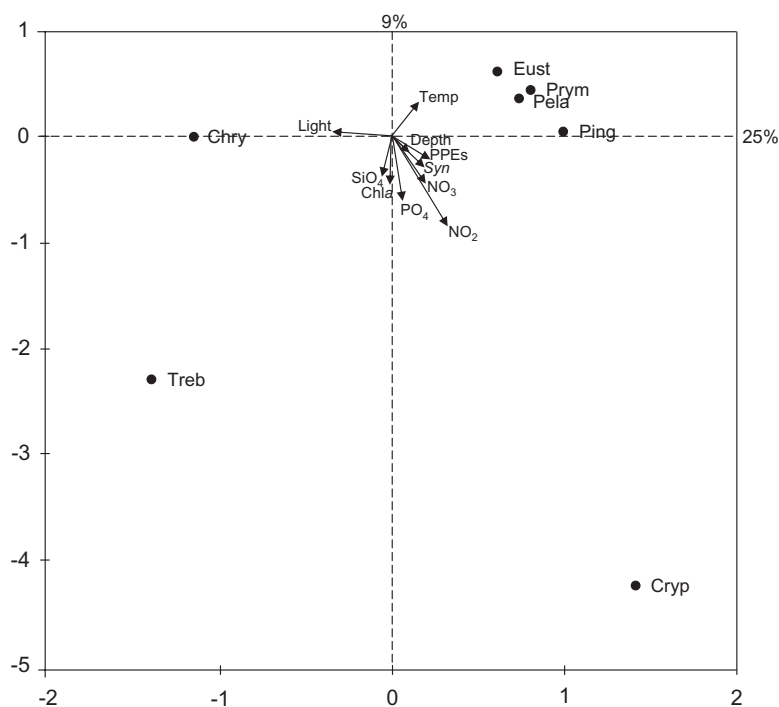


**Fig. 4.** CCA plot for PPE class distributions along AMT15 in relation to environmental variables, from dot blot hybridization results for classes: Prymnesiophyceae (Prym), Chrysophyceae (Chry), Cryptophyceae (Cryp), Pinguiphyceae (Ping), Pelagophyceae (Pela), Eustigmatophyceae (Eust) and Trebouxiophyceae (Treb). Arrows pointing in roughly the same direction indicate a high positive correlation, arrows crossing at right angles indicate a near-zero correlation, and arrows pointing in the opposite direction have a high negative correlation.

with the class-specific distribution patterns, in order of importance, were nitrite concentration, light intensity, temperature, abundance of photosynthetic eukaryotes, chlorophyll *a* concentration, depth, *Synechococcus* abundance, nitrate, phosphate and silicate concentrations, which explained 44% of the variation (Fig. 4). The *x*-axis explained 25% of this variation, and the *y*-axis a further 9%. Four additional axes (not shown) explained a further 5%, 3%, 1% and 1% respectively. Additional variables had very little effect on the amount of variation that could be explained. The CCA indicated that Chrysophyceae appear to be associated with higher light intensities, while temperature, silica, chlorophyll *a* and phosphate concentrations had a minimal relationship with the distribution of this class along AMT15. Pinguiphyceae are associated with low light intensities while the Trebouxiophyceae appear to be linked with lower temperatures, possibly reflecting the peak in abundance of this class below the thermocline in Northern and Southern gyres, and higher silicate and chlorophyll *a* concentrations. Conversely, the Eustigmatophyceae, Pelagophyceae and Prymnesiophyceae are linked with higher temperatures and lower silicate and chlorophyll *a* concentrations.

#### *Diversity of PPEs by phylogenetic analysis of nuclear and plastid rRNA gene sequences*

Coverage values for the 18S rRNA gene clone libraries were 72%, 55%, 69% and 69% for the northern temperate (station 1), upwelling (station 15), southern gyre (station

27) and southern temperate (station 33) libraries, respectively, whereas the 16S rRNA clone libraries had higher coverage values of 89%, 89%, 94% and 90% and the rarefaction index reached a plateau for these sites (see Fig. S2). Nuclear 18S rRNA gene clone libraries revealed a larger number of classes than the plastid 16S rRNA libraries (Table 1). However, most of these additional classes can be assigned to heterotrophic lineages. Hence, analysis of a much greater number of clones would be necessary to reveal the full extent of diversity in the 18S rRNA gene libraries.

The nuclear 18S rRNA gene libraries were dominated by sequences affiliated to the parasitic alveolates, Syndiniales. These sequences were analysed in Guillou and colleagues (2008) and hence are not reiterated here. Potentially photosynthetic classes accounted for only 11–33% of the clones in the 18S rRNA libraries. Of these, the most important classes appeared to be Prasinophyceae, Prymnesiophyceae and Chrysophyceae, which were present in all 18S rRNA gene libraries (Table 1). Within the Prasinophyceae, sequences related to *Bathycoccus* were particularly prevalent in the northern temperate clone library (station 1) (Fig. 5). Conversely, the plastid 16S rRNA gene libraries were dominated by sequences phylogenetically affiliated with the Prymnesiophyceae (Table 1). Sequences related to the Chrysophyceae were detected in all plastid 16S rRNA gene libraries, accounting for between 4% and 34% of clones, while those related to the Prasinophyceae accounted for 12% of clones in the northern temperate library, less than

**Table 1.** Composition and  $S_{\text{Chao1}}$  values of the nuclear 18S rRNA (N) and plastid 16S rRNA (P) clone libraries constructed at selected stations along AMT 15 (Fig. 1) at a depth corresponding to 55% surface light intensity.

Class	Number of clones (RFLP types)							
	1 N	P	15 N	15 P	27 N	27 P	33 N	33 P
<b>Prymnesiophyceae</b>	3 (1)	35 (5)	4 (2)	36 (3)	3 (1)	31 (1)	15 (3)	177 (11)
<b>Chrysophyceae</b>	1 (1)	46 (2)	5 (2)	3 (1)	15 (4)	11 (1)	3 (2)	12 (3)
<b>Cryptophyceae</b>	0	24 (3)	1 (1)	0	0	0	0	4 (1)
<b>Prasinophyceae</b>	0	0	3 (2)	0	0	0	12 (2)	2 (1)
<b>Mamiellophyceae</b>	64 (15)	27 (3)	2 (1)	0	8 (2)	0	1 (6)	0
<b>Dictyochophyceae</b>	1 (1)	14 (3)	0	0	0	0	0	3 (2)
<b>Bacillariophyceae</b>	0	0	0	0	0	0	4 (1)	0
<b>Pelagophyceae</b>	0	3 (1)	0	0	0	0	0	0
<b>Eustigmatophyceae</b>	0	3 (1)	0	0	0	0	0	0
<b>Chlorarachniophyceae</b>	0	0	2 (2)	0	0	0	1 (1)	0
<b>Dinophyceae</b>	0	3 (1)	0	0	0	0	0	0
Alveolata	101 (29)	0	124 (42)	0	76 (24)	0	166 (41)	0
Labyrinthulida	8 (1)	0	14 (9)	0	4 (2)	0	3 (3)	0
Pirsonia	0	0	4 (3)	0	0	0	0	0
Bicosoecida	0	0	1 (1)	0	0	0	0	0
Unknown Stramenopile	1 (1)	0	2 (2)	0	0	0	2 (1)	0
Acantharea	0	0	5 (3)	0	0	0	0	0
Taxapodida	0	0	1 (1)	0	0	0	0	0
Polycystinea	0	0	1 (1)	0	0	0	0	0
Apusozoa	0	0	1 (1)	0	0	0	0	0
Metazoa	26 (6)	0	8 (3)	0	0	0	2 (1)	0
Cyanobacteria	0	22 (2)	0	10 (1)	0	8 (1)	0	12 (3)
Heterotrophic bacteria	0	3 (1)	0	0	0	0	0	0
<b><math>S_{\text{Chao1}}</math> values (PPEs only)</b>	51.5	18.6	18.4	5.1	7	2	16.3	20.1

PPE classes are indicated in bold.

1% in the southern temperate library (2 clones out of 210) and were absent from the upwelling and southern gyre libraries.

When only the restriction fragment length polymorphism (RFLP) types from putative PPE classes were considered (i.e. excluding sequences related to prokaryotes from the plastid clone libraries and sequences related to heterotrophic classes from the nuclear libraries) the richness of the PPE community at each station could then be estimated using a non-parametric richness index,  $S_{\text{Chao1}}$ . The nuclear 18S rRNA gene library constructed from the northern temperate station had the highest richness ( $S_{\text{Chao1}}$  51.5), followed by the upwelling (18.4), southern temperate (16.3) and then the southern gyre station (7). For the plastid 16S rRNA gene libraries the southern temperate  $S_{\text{Chao1}}$  value was 20.1, followed by the northern temperate (18.6), upwelling (5.1) and the southern gyre (2) libraries.

Phylogenetic analysis of the nuclear and plastid rRNA Prymnesiophyceae sequences showed extensive diversity within the class (Figs 5 and 6), with nuclear 18S rRNA sequences falling within the Isochrysidales, Phaeocystidales and *Chrysochromulina* species from clade B2 within the order Prymnesiales (Edwardsen *et al.*, 2000). More RFLP types related to the Prymnesiophyceae were observed in the plastid than nuclear SSU rRNA gene libraries, with many sequences related to the Prymne-

siales, and fewer to the Isochrysidales, Phaeocystidales and Coccolithales together with a lineage containing no cultured representatives, close to the previously described Prym 16S-I and Prym 16S-II clades (Lepère *et al.*, 2009).

Phylogenetic relationships among the Chrysophyceae (Figs 5 and 6) revealed the presence of 18S rRNA sequences related to *Paraphysomonas* species, hence potentially from heterotrophic organisms. However, a sequence (env AMT\_27\_30m\_2) from the southern gyre library fell into group 'Marine B' (Shi *et al.*, 2009) and is therefore likely to belong to a photosynthetic organism, because sequences from this latter group although comprising only environmental sequences, derive from pigmented cells sorted by flow cytometry (Shi *et al.*, 2009). Similarly, plastid 16S rRNA sequences clustered largely separately from cultured representatives, which to our knowledge are virtually all larger than 3  $\mu\text{m}$  and mainly isolated from freshwater environments.

## Discussion

The flow cytometry data highlighted similar distributions patterns of PPEs, *Synechococcus* and *Prochlorococcus* to those observed in previous AMT cruises where *Prochlorococcus* dominated the oligotrophic gyres and



**Fig. 5.** Phylogenetic relationships among PPEs using nuclear 18S rRNA gene sequences and a neighbour-joining algorithm. Environmental sequences (approx. 1600 nucleotides in length) were added by ARB parsimony without a filter. Bootstrap analysis was performed using the ARB parsimony method (Ludwig *et al.*, 2004). Values > 70 and < 90% are marked with an open circle, values > 90% are marked with a filled circle. Environmental sequences from AMT15 are indicated in bold. Sequences representing the different RFLP types are also indicated [with the station number(s) where these RFLP types were found indicated in brackets; correction added on 26 January 2011, after first online publication: Fig. 5 was replaced due to misalignment of Marine A to C line bars].

*Synechococcus* and PPEs had peak numbers in the temperate and upwelling regions (Zubkov *et al.*, 1998; Heywood *et al.*, 2006). A peak of *Prochlorococcus* abundance of  $2 \times 10^5$  cells ml<sup>-1</sup> observed in the equatorial

southern oligotrophic gyre was the same as that observed on AMT3, sampled in the boreal autumn of 1996 (Zubkov *et al.*, 1998). Similarly, a distribution pattern of PPEs mirroring that of chlorophyll *a* concentrations, observed

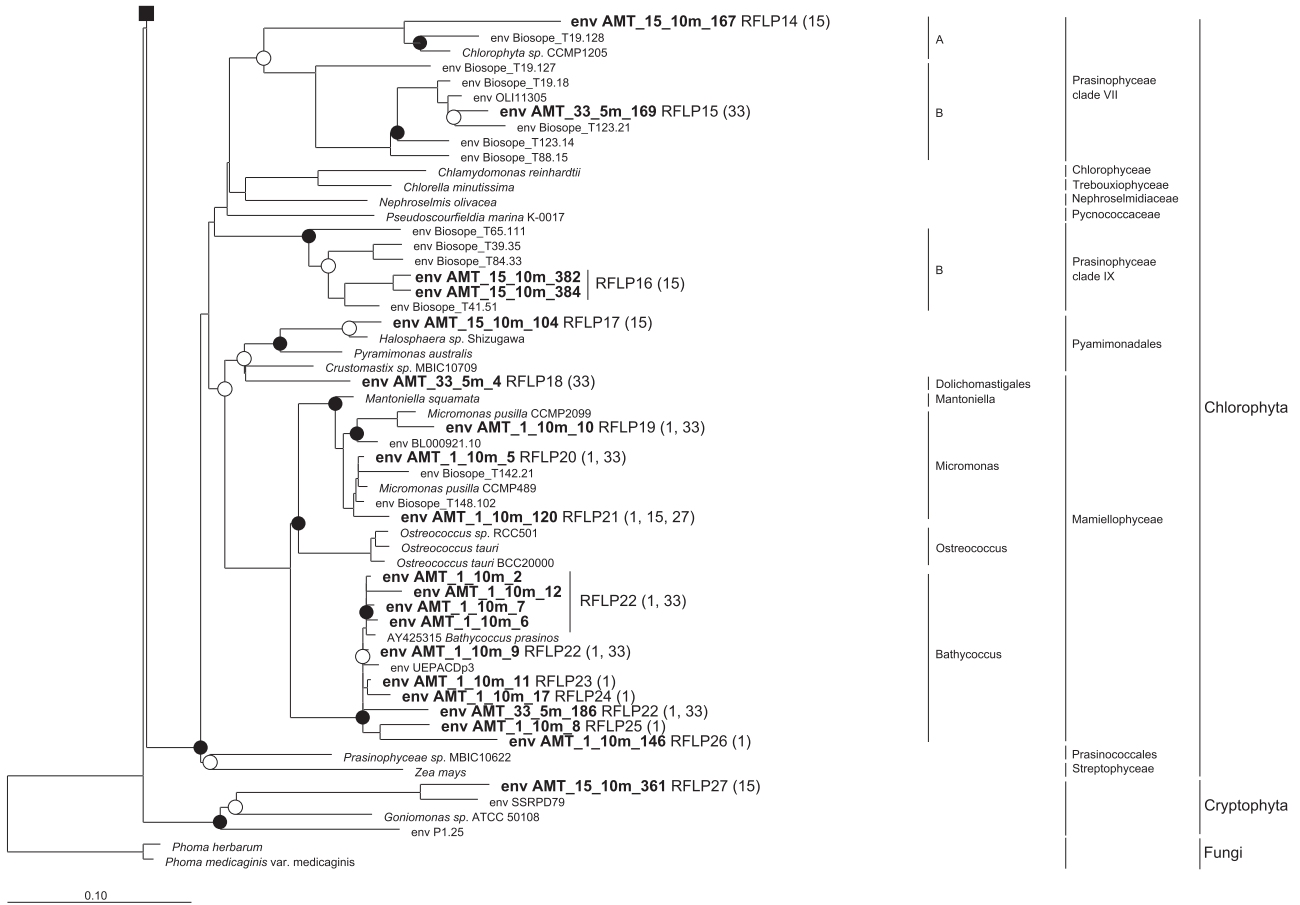


Fig. 5. cont.

during AMT13 and 14 (Tarran *et al.*, 2006), is also apparent here (Figs 2 and S1).

$S_{\text{chao1}}$  richness estimates for PPEs in both plastid and nuclear rRNA clone libraries were lowest at the southern gyre station but higher at northern and southern temperate stations, which to some extent is consistent with modelled predictions of the diversity of phytoplankton types in the euphotic zone within the same area covered by the AMT15 (see Barton *et al.*, 2010). These predictions are thought to reflect a prolonged coexistence of multiple phytoplankton with comparable fitness (Barton *et al.*, 2010).

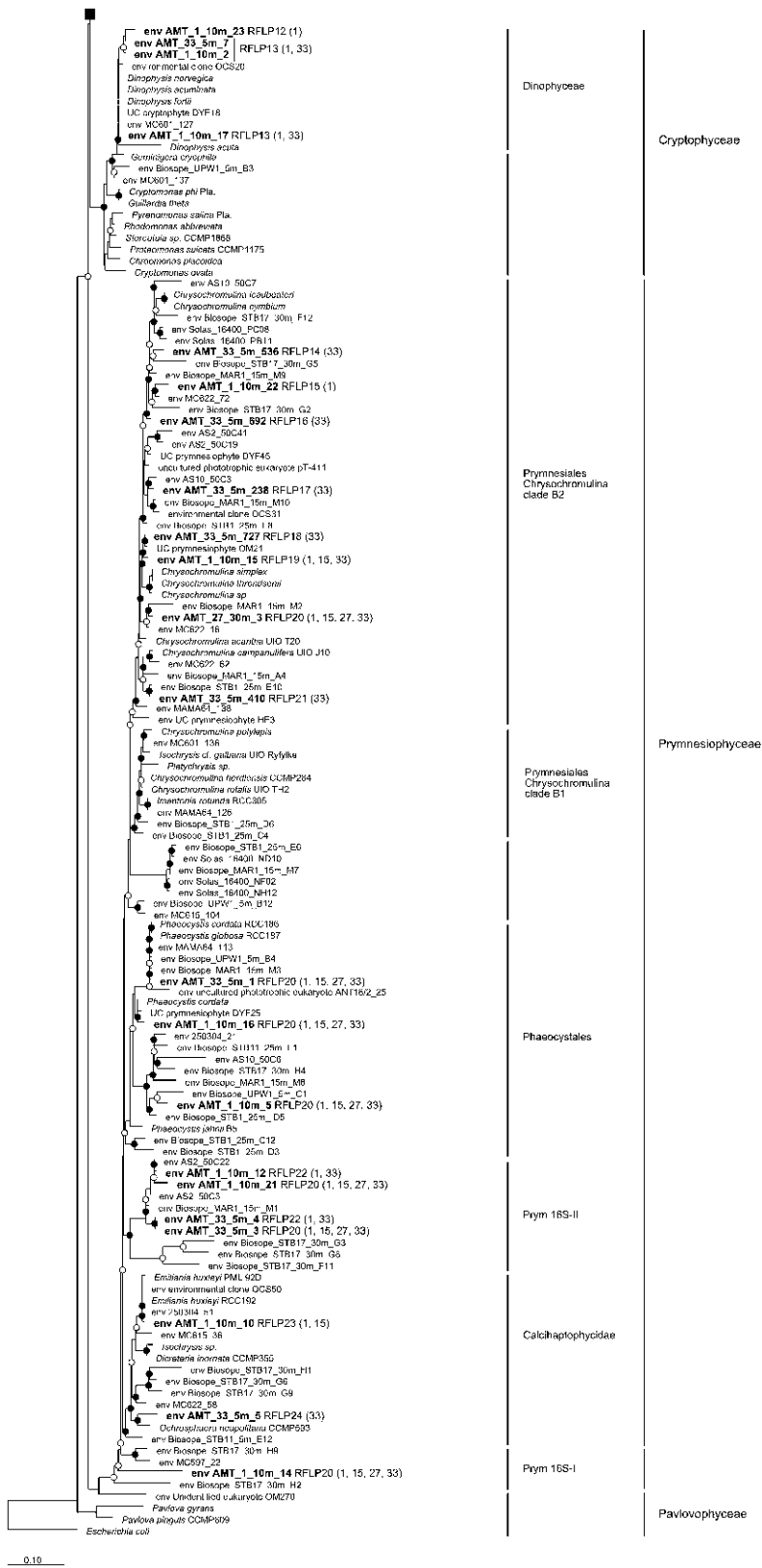
Analysis of the dot blot hybridization data showed that the sum of the class-specific relative hybridization values rarely reached 100%. This may indicate that sequences from other classes have been amplified but were not targeted by the probes used. This is particularly notable for samples at depths corresponding to the lowest light intensity levels sampled, where photosynthetic cells may be much less numerous. Although generally not abundant, some PPE classes were found in the plastid clone libraries for which dot blot hybridization probes were not available, namely Dictyochophyceae, Mamiellophyceae,

Dinophyceae and Bacillariophyceae. Furthermore, while the marine algal plastid PCR approach significantly enriches PPE sequences, some cyanobacterial and heterotrophic bacterial sequences were still present in these clone libraries, albeit in low numbers.

Despite the low taxonomic resolution of dot blot hybridization analyses i.e. targeting the class level, and thus potentially missing the large diversity that is now apparent for some classes, e.g. Prymnesiophyceae (Liu *et al.*, 2009) or Prasinophyceae, the latter including specialized ecotypes in some genera (Rodríguez *et al.*, 2005; Viprey *et al.*, 2008), CCA analysis showed that measured variables could still explain 48% of the variation in dot blot hybridization data. The remaining variation, i.e. which could not be explained by the measured variables, may be explained by biotic factors such as viral lysis and predator abundance/grazing rates. Certainly, marine viruses are known to be an important controlling factor over their host communities (Fuhrman, 1999) and zooplankton grazing has been shown to influence small eukaryote assemblages in freshwater and marine habitats (Lepère *et al.*, 2006; Baudoux *et al.*, 2008). Furthermore,



Fig. 6. cont.



it has recently been shown that in the North Atlantic Ocean PPEs perform unexpectedly high rates of bacterivory (Zubkov and Tarran, 2008). This suggests that the targeted PPEs may be less dependent on the availability of inorganic nutrients than previously thought and may also result in PPE distribution patterns being influenced by the availability of bacterioplankton prey.

The dominance of sequences related to the Prymnesiophyceae in the plastid clone libraries constructed here, as well as their high relative hybridization values, is in good agreement with previous pigment studies from the study region, which found 19'-hexanoyloxyfucoxanthin (a diagnostic pigment for this class) to be the dominant photosynthetic pigment along the AMT2-5 transects (Gibb *et al.*, 2000). While larger members of the Prymnesiophyceae have been well studied, playing critical roles in elemental cycling, e.g. *Emiliana huxleyi* in S cycling (see Green and Leadbeater, 1994) much less is known of pico-sized representatives. However, a recent study in the subtropical and tropical northeast Atlantic Ocean, using FISH analyses coupled to radiotracer uptake and flow cytometric sorting, found prymnesiophytes < 3 µm in size to be major players in CO<sub>2</sub> fixation (Jardillier *et al.*, 2010). The recent work of Liu and colleagues (2009) and Cuvelier and colleagues (2010) also emphasizes the importance, in terms of abundance and biomass, of picoprymnesiophytes in the world's oceans. Unfortunately, most cultured representatives are generally larger than this, with the exception of *Imantonia rotunda* and *Phaeocystis cordata*, which are observed to fall within the 'pico' size range for at least part of their life cycle (Vaulot *et al.*, 2008). Indeed, sequences clustering near to these species were observed in both the nuclear and plastid rRNA gene phylogenies (see Figs 5 and 6, respectively). Both approaches also yielded sequences phylogenetically related to *Chrysochromulina* species but there were also several plastid sequences forming a lineage with no close cultured representatives.

The other key class, the Chrysophyceae, has traditionally been observed only at low abundance in microscopy studies performed on marine samples (Thronsdon, 1996; Novarino *et al.*, 1997). However, sequences related to both heterotrophic and photosynthetic Chrysophyceae have recently been obtained from a range of marine environments, including the Sargasso Sea (Not *et al.*, 2007a) and South East Pacific Ocean (Shi *et al.*, 2009), while both clone library and dot blot hybridization data have shown photosynthetic representatives of this class reaching high relative proportions in the Arabian Sea (Fuller *et al.*, 2006a,b), Mediterranean Sea (McDonald *et al.*, 2007) and south-east Pacific Ocean (Lepère *et al.*, 2009). A temporal study of PPE community structure off the coast of Naples in the Mediterranean Sea found Chrysophyceae dynamics to be seasonal, this class being abun-

dant during the summer months (McDonald *et al.*, 2007). The Chrysophyceae distribution along AMT15 was found to be linked with elevated light levels, and not influenced by temperature (Fig. 4). Thus, the former variable may have governed the seasonality observed in the Gulf of Naples. Within the Chrysophyceae, the order Parmales is essentially the only documented marine group, comprising solitary cells 2–5 µm in diameter each with a single chloroplast and a silicified cell wall but lacking cultured representatives (Booth and Marchant, 1987; Bravo-Sierra and Hernández-Becerril, 2003). However, CCA analysis showed no relationship between Si concentration and Chrysophyceae proportions (Fig. 4) indicating this factor is unlikely to influence the distribution of this class along the AMT, or at least is not a critical limiting factor.

The relatively low abundance of Cryptophyceae, as assessed both by dot blot hybridization analysis and clone library construction performed here, differs with other molecular studies, which have reported members of the Cryptophyceae to be as abundant as the Prymnesiophyceae at both a Mediterranean Sea coastal site (McDonald *et al.*, 2007) and across a transect in the South East Pacific Ocean (Lepère *et al.*, 2009). Cryptophyceae have also been shown to be well represented in nuclear SSU clone libraries from a coastal site in the English Channel (Romari and Vaulot, 2004). In contrast, during a transect of the Arabian Sea this class was generally restricted to higher-nutrient coastal stations at 20–30 m depths off the coast of Oman (Fuller *et al.*, 2006b). The CCA revealed the abundance of this class along AMT15 was related to nutrient concentration (Fig. 4), with peak relative hybridization values occurring in the mesotrophic upwelling region. For the Pinguicophyceae, Trebouxiophyceae and Eustigmatophyceae peak relative hybridization values reached between 2% and 15%, generally at depth. This is similar to their distribution in the Arabian Sea as also indicated by dot blot hybridization analysis (Fuller *et al.*, 2006b).

Despite members of the Pelagophyceae being isolated into culture relatively frequently (e.g. from the Pacific gyre (Le Gall *et al.*, 2008), the generally low abundance of members of the class along AMT15 is consistent with their rarity in environmental clone libraries of nuclear rRNA genes (see Vaulot *et al.*, 2008) and from previous dot blot hybridization analyses (e.g. see McDonald *et al.*, 2007). However, clones related to the Pelagophyceae have been found to be well represented in some plastid 16S rRNA gene clone libraries from the Arabian Sea (Fuller *et al.*, 2006a).

The nuclear SSU rRNA gene libraries indicated a significant contribution of Prasinophyceae to the PPE community along AMT15, although this class was not detected by dot blot hybridization analysis and was rare in the plastid rRNA gene libraries. This rarity may be a result of

PCR bias against some prasinophyte groups, which has been previously documented for the plastid rRNA gene primers used here (McDonald *et al.*, 2007). Such bias may explain the lower richness ( $S_{\text{Chao1}}$ ) values of the plastid clone libraries compared with their nuclear counterparts. Extensive Prasinophyceae diversity is observed in the nuclear SSU rRNA gene phylogenies (Fig. 5), with sequences falling within clades I, VII and IX (see Viprey *et al.*, 2008 for clade designations) and Mamiellophyceae ( $\equiv$  Prasinophyceae clade II) (Marin and Melkonian, 2010). In particular, Mamiellophyceae sequences related to the genera *Bathycoccus* and *Micromonas* were particularly prevalent in the northern temperate station 1 library. This latter observation is consistent with previous studies [see Not *et al.*, 2004; 2008; Worden and Not (2008)] that have shown members of the Mamiellophyceae dominate coastal waters but are not abundant in open ocean waters. Indeed, Jardillier and colleagues (2010) found < 5% of prasinophyte cells using FISH in flow sorted PPE populations from a region in the Atlantic adjacent to the Cape Verde Islands (and hence in a similar region to station 15 from this study). Phylogenetic analysis of plastid 16S rRNA gene sequences (Fig. 6) revealed three sequences related to the Mamiellophyceae and a single sequence related to Pras16S-VIII (Lepère *et al.*, 2009), a novel lineage currently containing no cultured counterparts and potentially 'equivalent' to nuclear clade IX (Viprey *et al.*, 2008). The latter clade appears not be abundant along AMT15 as only two 18S rRNA clones related to clade IX were obtained. Certainly, the fact that plastid sequences attributable to the Pras16S-VIII clade are well represented in libraries constructed from the South East Pacific (Lepère *et al.*, 2009) suggests that at least this prasinophyte clade is not obviously excluded by the plastid primer set used here.

## Conclusions

We have presented here a large molecular data set that begins to elucidate the community structure and distribution of key members of the eukaryotic phytoplankton community, namely the PPEs, along a c. 13 500 km transect in the Atlantic Ocean, and which complements previous work performed on their pico-sized photosynthetic prokaryote counterparts (see Zwirgmaier *et al.*, 2007).

The PPE community along AMT15 was dominated by members of the classes Prymnesiophyceae and Chrysophyceae, with smaller contributions from Prasinophyceae, Cryptophyceae, Pelagophyceae, Pinguicophyceae, Trebouxiophyceae and Eustigmatophyceae. Neither dominant class is traditionally considered to be an important member of the marine PPE community: Prymnesiophyceae are generally known to be larger than 3  $\mu\text{m}$  in diameter, although recent studies have begun to reveal

the importance of this size class (McDonald *et al.*, 2007; Liu *et al.*, 2009; Cuvelier *et al.*, 2010; Jardillier *et al.*, 2010), while photosynthetic chrysophytes, at least as described cultures, are mostly known from freshwater systems (Andersen, 2007). These two major classes displayed strikingly complementary distribution patterns, prymnesiophytes dominating northern gyre waters while chrysophytes dominated northern temperate, southern gyre and equatorial regions, although some of this variation may be due to the different seasons sampled in the northern and southern hemispheres. Interestingly, shifts in abundance of major prokaryotic lineages, e.g. SAR11, have also been observed between the two Atlantic gyres (Schattenhofer *et al.*, 2009). Despite Chrysophyceae being associated with elevated light intensities Prymnesiophyceae were not obviously associated with any measured variable. Indeed, over half of the variation in PPE class distribution patterns could not be explained by the measured parameters, thus factors underlying their distributions have yet to be identified. Phylogenetic analysis showed that both of these key classes contain lineages for which no or few cultured counterparts are available. Future culturing efforts are thus essential to isolate and further characterize these potentially important primary producers. Also, further investigations are required to understand the distribution of PPEs at the global scale as well as their  $\text{CO}_2$  fixation activity, which is critical to a full understanding of C cycling in the upper ocean.

## Experimental procedures

### Sampling

Water samples were collected in September/October 2004 during the AMT15 cruise aboard the RRS *Discovery*. Samples were obtained from six discrete depths (surface, 55%, 33%, 14%, 1% and 0.1% surface light intensity) at 21 stations along the cruise track (Fig. 1) with a rosette of 20 l Niskin bottles. Light conditions correspond to the total incident PAR, measured using a Chelsea PAR Sensor (UWIRR). Temperature was measured using a SBE 3P temperature sensor and a digiquartz temperature compensated pressure sensor. For DNA extraction, 10 l of seawater was filtered first through a 47 mm diameter, 3  $\mu\text{m}$  pore size polycarbonate filter (Millipore MCE MF) and then onto a 47 mm diameter, 0.45  $\mu\text{m}$  pore size polysulfone filter (Supor450, Gelman Sciences, Ann Arbor, Mich) under gentle vacuum (10 mm Hg). Use of a 3  $\mu\text{m}$  pore-size filter conforms with what is currently widely used methodology to select the picoeukaryote community (see Vaulot *et al.*, 2008) although we cannot exclude that cells larger than 3  $\mu\text{m}$ , or plastids from lysed cells, may have passed through this pore-size filter. The filters were transferred into 5 ml cryotubes containing 3 ml of DNA lysis buffer (0.75 M sucrose, 400 mM NaCl, 20 mM EDTA, 50 mM Tris pH 9.0) and stored at  $-80^\circ\text{C}$  until DNA extraction. DNA was subsequently extracted from the filters as described previously (Fuller *et al.*, 2003).

### Nutrient analysis

Micromolar nitrate, nitrite, silicate and phosphate concentrations were determined using a five-channel Bran and Luebbe segmented flow colorimetric autoanalyser as described previously (Zwirgmaier *et al.*, 2007). Concentrations mentioned in the text are average values from seawater samples collected from surface waters down to 0.1% light levels unless otherwise stated.

### Flow cytometric analysis

Photosynthetic picoeukaryotes, *Prochlorococcus* and *Synechococcus* were identified and enumerated using flow cytometry (FACSort, Beckton Dickinson, Oxford, UK) by their characteristic pigment autofluorescence and size. The flow rate was calculated by adding a known concentration of 0.5 mm yellow-green fluorescent latex beads (Polysciences, Eppelheim, Germany) as an internal standard (Zubkov and Burkill, 2006). Flow cytometry data were processed using CellQuest software (Beckton Dickinson, Oxford, UK).

### Polymerase chain reaction amplification

Polymerase chain reaction amplification of the 16S rRNA gene from environmental DNA and from control strains for dot blot hybridization and/or clone library construction used the algal plastid biased primer PLA491F (Fuller *et al.*, 2006a) coupled with the general oxygenic phototroph primer OXY1313R (West *et al.*, 2001) to give an approximately 830 bp PCR product.

For dot blot hybridization analysis PCR amplification was carried out using a hot-start method in a final volume of 50  $\mu$ l, containing 1 mg ml<sup>-1</sup> BSA, 1  $\times$  enzyme buffer, 1.2 mM MgCl<sub>2</sub>, 200  $\mu$ M dNTPs, 0.8  $\mu$ M primers and 2.5 U *Taq* polymerase. Amplification conditions consisted of 30 cycles of 95°C for 30 s, 60°C for 30 s and 72°C for 40 s, and a final extension step of 72°C for 6 min. For plastid clone library construction the same PCR conditions were used with the exception of PCR primers (0.2  $\mu$ M final concentration) and *Taq* polymerase (1.2 U).

PCR amplification of the 18S rRNA gene used the general eukaryote primer pair 7F and 1534R (Moon-van der Staay *et al.*, 2001) in a total volume of 50  $\mu$ l, with 1 mg ml<sup>-1</sup> BSA, 1  $\times$  enzyme buffer, 1.5 mM MgCl<sub>2</sub>, 200  $\mu$ M dNTPs, 0.5  $\mu$ M primers and 2.5 U HotStarTaq® (Qiagen). The amplification conditions were 95°C for 15 min followed by 35 cycles of 95°C for 1 min, 57°C for 1 min 30 s and 72°C for 1 min 30 s, and a final extension step of 72°C for 10 min.

### Dot blot hybridization

Dot blot hybridization conditions for the various marine algal class-specific oligonucleotides were optimized previously (Fuller *et al.*, 2006b). Algal cultures used as controls were the same as those used by Fuller and colleagues (2006b) and were obtained from the Roscoff Culture Collection (RCC, <http://www.sb-roscoff.fr/Phyto/RCC/>) and the Provasoli-Guillard National Center for Culture of Marine Phytoplankton (CCMP, <https://ccmp.bigelow.org/>). 16S rDNA amplicons from

AMT environmental DNA and control strains, obtained by PCR as described above, were purified, blotted onto nylon membranes and hybridized to algal class-specific oligonucleotide probes, following the method of Fuller and colleagues (2003). The oligonucleotide probes used were: CHLA768, CHRY1037, CRYP862, EUST985, PAVL665, PELA1035, PING1024, PRAS826, PRYM666 and TREB708 targeting the plastids of Chlorarachniophyceae, Chrysoophyceae, Cryptophyceae, Eustigmatophyceae, Pavlovophyceae, Pelagophyceae, Pinguicophyceae, Prasinophyceae clade VI (Prasinococcales), Prymnesiophyceae and Trebouxiophyceae respectively (Fuller *et al.*, 2006b). Final wash (or dissociation) temperatures (Td) for each probe were determined empirically (Fuller *et al.*, 2006b), following a previously described method (Fuller *et al.*, 2003). Hybridization was quantified by using a Fujifilm FLA-5000 phosphorimager and Total Laboratory software (Phoretix). Hybridization of the PPE class-specific probes relative to that of all PCR amplicons amplified by the PLA491F-OXY1313R primer pair was calculated according to the equation below:

$$\text{Relative hybridization (\%)} = \left[ \left( \frac{S_{env}}{E_{env}} \right) \cdot \left( \frac{S_{con}}{E_{con}} \right)^{-1} \right] \times 100$$

where *S<sub>env</sub>* and *E<sub>env</sub>* represent hybridization to environmental DNA of the specific and eubacterial probes, respectively; *S<sub>con</sub>* and *E<sub>con</sub>* are the slopes of the specific and eubacterial probe-binding curves, respectively, calculated by hybridizing each probe to dilution series of homogenous control DNA. The relative hybridization of a given specific probe compared with that of the eubacterial probe to the control DNA was averaged where more than one control DNA was used. Any sample giving a signal above 2% was considered above background. Three replicates were analysed for each algal class-specific oligonucleotide probe and for each sample. Values given in the figures and text correspond to the mean of these three replicates. The standard deviation for all samples was 3.9%.

### Construction of plastid and nuclear rRNA clone libraries

Seawater samples for subsequent construction of 16S and 18S rRNA gene clone libraries were collected at a depth corresponding to 55% surface light intensity at four separate stations along AMT15: station 1 in the northern temperate region (48°44'N, 07°50'W, 10 m depth), station 15 in the upwelling region (17°37'N, 20°57'W, 10 m depth), station 27 in the southern gyre (23°33'S, 17°29'W, 30 m depth) and station 33 in the southern temperate region (37°50'S, 1°14'E, 5 m depth) (see Fig. 1 and Table S1). Environmental DNA extraction and PCR amplification were performed as described above. PCR products were cloned into the TA vector pCR2.1-TOPO (Invitrogen) and screened by RFLP after digestion with *Hae*III and *Eco*RI (Fermentas) or *Hae*III alone, for plastid and nuclear rRNA products respectively. Clones with the same RFLP pattern were considered members of the same operational taxonomic unit and at least one member of each operational taxonomic unit was sequenced for phylogenetic analysis. Sequencing was carried out using an ABI PRISM 3130xl Genetic Analyser® (Applied Biosystems) at the NERC Biomolecular analysis

facility (NBAF) in Edinburgh. A third sequencing primer, 528F (Elwood *et al.*, 1985) facilitated completion of the near full-length 18S rRNA gene.

### Phylogenetic analysis

Sequences were assembled using Seqman software (DNASTAR) and initially checked for the presence of chimeric artefacts using the Check Chimera programme within the Ribosomal Database Project (Cole *et al.*, 2003). Sequences were aligned using ARB software (Ludwig *et al.*, 2004) and manually rechecked for the presence of chimeras by assessing the phylogenetic position of each half of the sequence in ARB. Sequences considered to be chimeric were excluded from further analysis. Phylogenetic trees were produced using ARB with a neighbour-joining algorithm with Jukes-Cantor correction. Short environmental sequences (< 1000 bp) were added by ARB parsimony. For 16S rRNA gene sequences, a maximum frequency filter for plastids was used. Bootstrap analysis was performed with the ARB parsimony bootstrap algorithm with independent nearest neighbour interchange. 16S and 18S rRNA gene sequences of potentially photosynthetic classes have been deposited in GenBank under accession numbers GQ863739-GQ863780, HQ401020, HM437227-HM437230 (plastid) or GQ863798-GQ863827, HQ132224-HQ132226 (nuclear). Nuclear 18S rRNA gene sequences pertaining to the alveolates (GenBank accession no. EU780589-EU780636) have been published elsewhere (Guillou *et al.*, 2008), while those representing other heterotrophic lineages can be found under accession numbers GQ863781-GQ863797.

### Statistical analyses

We performed CCA of diversity data using the vegan package (Legendre and Legendre, 1998) within the R software (<http://cran.r-project.org>) to explore relationships between the explanatory variables (environmental parameters) and the response variables [i.e. diversity data and specifically the PLA491F-OXY1313R dot blot relative hybridization values (%)]. Environmental parameters included in the analysis were concentrations of nitrate, nitrite, phosphate, silicate, dissolved oxygen, salinity, light intensity, depth, temperature, abundances of *Prochlorococcus*, *Synechococcus* and photosynthetic eukaryotes and chl *a* concentration. CCA plots were drawn using R software with biplot values of the environmental variables and eigenvectors of dot blot hybridization data group scores.

Rarefaction analyses were carried out using Analytic Rarefaction 1.3 (Holland, 2003). Coverage values were calculated for each clone library as an estimate of the proportion of RFLP types from a sample that are represented in a clone library. This was calculated using  $C = 1 - (n_1/N)$  where  $n_1$  is the number of RFLP types appearing in a library and  $N$  is the total number of clones analysed in the library. The non-parametric richness estimate,  $S_{\text{Chao1}}$  (Hughes *et al.*, 2001), was calculated as follows:

$$S_{\text{Chao1}} = S_{\text{obs}} + F_1^2 / [2 \times (F_2 + 1)] - (F_1 \times F_2) / [2 \times (F_2 + 1)]$$

where  $S_{\text{obs}}$  = the number of different RFLP types observed.

$F_1$  = the number of RFLP types to which only one clone was assigned.

$F_2$  = the number of RFLP types to which only two clones were assigned.

### Acknowledgements

The authors would like to thank the crew of the RRS *Discovery* for excellent logistical support on AMT15. We also thank Katrin Zwirgmaier for extraction of the DNA samples used in this work and Jane Heywood for providing flow cytometry data. This study was supported by the UK Natural Environment Research Council via a PhD studentship award to AK and NERC Grant NE/C003160/1 to D.J.S and M.V.Z. This is contribution number 191 of the AMT programme.

### References

- Aiken, J., and Bale, A.J. (2000) An introduction to the Atlantic Meridional Transect (AMT) programme. *Prog Oceanogr* **45**: 251–256.
- Aiken, J., Pradhan, Y., Barlow, R., Lavender, S., Poulton, A., Holligan, P., and Hardman-Mountford, N. (2009) Phytoplankton pigments and functional types in the Atlantic Ocean: a decadal assessment, 1995–2005. *Deep Sea Res Part II Top Stud Oceanogr* **56**: 899–917.
- Andersen, R.A. (2007) Molecular systematics of the Chryso-phyceae and Synurophyceae. In *Unravelling the Algae: The Past, Present and Future of Algal Systematics*. Brodie, J., and Lewis, J. (eds). Boca Raton, FL, USA: CRC Press, pp. 283–311.
- Barton, A.D., Dutkiewicz, S., Flierl, G., Bragg, J., and Follows, M.J. (2010) Patterns of diversity in marine phytoplankton. *Science* **327**: 1509–1511.
- Baudoux, A.C., Veldhuis, M.J.W., Noordeloos, A.A.M., van Noort, G., and Brussaard, C.P.D. (2008) Estimates of virus- vs. grazing induced mortality of picophytoplankton in the North Sea during summer. *Aquat Microb Ecol* **52**: 69–82.
- Booth, B.C., and Marchant, H.J. (1987) Parmales, a new order of marine chrysophytes, with descriptions of three new genera and seven new species. *J Phycol* **23**: 245–260.
- Bravo-Sierra, E., and Hernández-Becerril, D.U. (2003) Parmales (Chrysophyceae) from the Gulf of Tehuantepec, Mexico, including the description of a new species, *Tetraparma insecta* sp. nov., and a proposal to the taxonomy of the group. *J Phycol* **39**: 577–583.
- Cole, J.R., Chai, B., Marsh, T.L., Farris, R.J., Wang, Q., Kulam, S.A., *et al.* (2003) The Ribosomal Database Project (RDP-II): previewing a new autoaligner that allows regular updates and the new prokaryotic taxonomy. *Nucleic Acids Res* **31**: 442–443.
- Cuvelier, M.L., Allen, A.E., Monier, A., McCrow, J.P., Messié, M., Tringe, S.G., *et al.* (2010) Targeted metagenomics and ecology of globally important uncultured eukaryotic phytoplankton. *Proc Natl Acad Sci USA* **107**: 14679–14684.
- Díez, B., Pedrós-Alió, C., and Massana, R. (2001) Study of genetic diversity of eukaryotic picoplankton in different oceanic regions by small-subunit rRNA gene cloning and sequencing. *Appl Environ Microbiol* **67**: 2932–2941.

- Edwardsen, B., Eikrem, W., and Green, J.C. (2000) Phylogenetic reconstruction of the Haptophyta inferred from 18S ribosomal DNA sequences and available morphological data. *Phycologia* **39**: 19–35.
- Elwood, H.J., Olsen, G.J., and Sogin, M.L. (1985) The small subunit ribosomal RNA gene sequences from the hypotrichous ciliates *Oxytricha nova* and *Stylonychia pustulata*. *Mol Biol Evol* **2**: 399–410.
- Field, C.B., Behrenfeld, M.J., Randerson, J.T., and Falkowski, P. (1998) Primary production of the biosphere: integrating terrestrial and oceanic components. *Science* **281**: 237–240.
- Fuhrman, J.A. (1999) Marine viruses and their biogeochemical and ecological effects. *Nature* **399**: 541–548.
- Fuller, N.J., Marie, D., Partensky, F., Vaulot, D., Post, A.F., and Scanlan, D.J. (2003) Clade-specific 16S ribosomal DNA oligonucleotides reveal the predominance of a single marine *Synechococcus* clade throughout a stratified water column in the Red Sea. *Appl Environ Microbiol* **69**: 2430–2443.
- Fuller, N.J., Campbell, C., Allen, D.J., Pitt, F.D., Zwirgmaier, K., Le Gall, F., *et al.* (2006a) Analysis of photosynthetic picoeukaryote diversity at open ocean sites in the Arabian Sea using a PCR biased towards marine algal plastids. *Aquat Microb Ecol* **43**: 79–93.
- Fuller, N.J., Tarran, G.A., Cummings, D.G., Woodward, E.M.S., Orcutt, K.M., Yallop, M., *et al.* (2006b) Molecular analysis of photosynthetic picoeukaryote community structure along an Arabian Sea transect. *Limnol Oceanogr* **51**: 2502–2514.
- Gibb, S.W., Barlow, R.G., Cummings, D.G., Rees, N.W., Trees, C.C., and Holligan, P. (2000) Surface phytoplankton pigment distributions in the Atlantic Ocean: an assessment of basin scale variability between 50°N and 50°S. *Prog Oceanogr* **45**: 339–368.
- Green, J.C., and Leadbeater, B.S.C. (eds) (1994) *The Haptophyte Algae*. Oxford, UK: Oxford University Press.
- Guillou, L., Viprey, M., Chambouvet, A., Welsh, R.M., Kirkham, A.R., Massana, R., *et al.* (2008) Widespread occurrence and genetic diversity of marine parasitoids belonging to *Syndiniales* (*Alveolata*). *Environ Microbiol* **10**: 3349–3365.
- Heywood, J.L., Zubkov, M.V., Tarran, G.A., Fuchs, B.M., and Holligan, P.M. (2006) Prokaryoplankton standing stocks in oligotrophic gyre and equatorial provinces of the Atlantic Ocean: evaluation of inter-annual variability. *Deep Sea Res Part II Top Stud Oceanogr* **53**: 1530–1547.
- Holland, S. (2003) *UGA Stratigraphy Lab* [WWW document]. URL <http://www.uga.edu/~strata/software/>.
- Hooker, S.B., Rees, N.W., and Aiken, J. (2000) An objective methodology for identifying oceanic provinces. *Prog Oceanogr* **45**: 313–338.
- Hughes, J.B., Hellmann, J.J., Ricketts, T.H., and Bohannon, B.J.M. (2001) Counting the uncountable: statistical approaches to estimating microbial diversity. *Appl Environ Microbiol* **67**: 4399–4406.
- Jardillier, L., Zubkov, M.V., Pearman, J., and Scanlan, D.J. (2010) Significant CO<sub>2</sub> fixation by small prymnesiophytes in the subtropical and tropical northeast Atlantic Ocean. *ISME J* **4**: 1180–1192.
- Le Gall, F., Rigaut-Jalabert, F., Marie, D., Garczarek, L., Viprey, M., Godet, A., and Vaulot, D. (2008) Picoplankton diversity in the South-East Pacific Ocean from cultures. *Biogeosciences* **5**: 203–214.
- Legendre, P., and Legendre, L. (1998) *Numerical Ecology*, 2nd edn. Amsterdam, The Netherlands: Elsevier Science BV.
- Lepère, C., Boucher, D., Jardillier, L., Domaizon, I., and Debroas, D. (2006) Succession and regulation factors of small eukaryote community composition in a lacustrine ecosystem (Lake Pavin). *Appl Environ Microbiol* **72**: 2971–2981.
- Lepère, C., Vaulot, D., and Scanlan, D.J. (2009) Photosynthetic picoeukaryote community structure in the South East Pacific Ocean encompassing the most oligotrophic waters on Earth. *Environ Microbiol* **11**: 3105–3117.
- Li, W.K.W. (1994) Primary production of prochlorophytes, cyanobacteria, and eucaryotic ultraphytoplankton: measurements from flow cytometric sorting. *Limnol Oceanogr* **39**: 169–175.
- Liu, H., Probert, I., Uits, J., Claustre, H., Aris-Brosou, S., Frada, M., *et al.* (2009) Extreme diversity in noncalcifying haptophytes explains a major pigment paradox in open oceans. *Proc Natl Acad Sci USA* **106**: 12803–12808.
- Longhurst, A.R. (2007) *Ecological Geography of the Sea*, 2nd edn. Amsterdam, The Netherlands: Elsevier Academic Press.
- Lovejoy, C., Massana, R., and Pedrós-Alió, C. (2006) Diversity and distribution of marine microbial eukaryotes in the Arctic Ocean and adjacent seas. *Appl Environ Microbiol* **72**: 3085–3095.
- Ludwig, W., Strunk, O., Westram, R., Richter, L., Meier, H., Yadhukumar, *et al.* (2004) ARB: a software environment for sequence data. *Nucl Acids Res* **32**: 1363–1371.
- McDonald, S.M., Sarno, D., Scanlan, D.J., and Zingone, A. (2007) Genetic diversity of eukaryotic ultraphytoplankton in the Gulf of Naples during an annual cycle. *Aquat Microb Ecol* **50**: 75–89.
- Marañón, E., Holligan, P.M., Barciela, R., Gonzalez, N., Mourino, B., Pazo, M.J., *et al.* (2001) Patterns of phytoplankton size structure and productivity in contrasting open-ocean environments. *Mar Ecol Prog Ser* **216**: 43–56.
- Marin, B., and Melkonian, M. (2010) Molecular phylogeny and classification of the Mamiellophyceae class. nov. (Chlorophyta) based on sequence comparisons of the nuclear- and plastid-encoded rRNA operons. *Protist* **161**: 304–336.
- Massana, R., Balagué, V., Guillou, L., and Pedrós-Alió, C. (2004) Picoeukaryotic diversity in an oligotrophic coastal site studied by molecular and culturing approaches. *FEMS Microbiol Ecol* **50**: 231–243.
- Moon-van der Staay, S.Y., De Watchter, R., and Vaulot, D. (2001) Oceanic 18S rDNA sequences from picoplankton reveal unsuspected eukaryotic diversity. *Nature* **409**: 607–610.
- Not, F., Simon, N., Biegala, I.C., and Vaulot, D. (2002) Application of fluorescent in situ hybridization coupled with tyramide signal amplification (FISH-TSA) to assess eukaryotic picoplankton composition. *Aquat Microb Ecol* **28**: 157–166.
- Not, F., Latasa, M., Marie, D., Cariou, T., Vaulot, D., and Simon, N. (2004) A single species *Micromonas pusilla* (Prasinophyceae), dominates the eukaryotic picoplankton

- in the Western English Channel. *Appl Environ Microbiol* **70**: 4064–4072.
- Not, F., Gausling, R., Azam, F., Heidelberg, J.F., and Worden, A.Z. (2007a) Vertical distribution of eukaryotic diversity in the Sargasso Sea. *Environ Microbiol* **9**: 1233–1252.
- Not, F., Valentin, K., Romari, K., Lovejoy, C., Massana, R., Töbe, K., et al. (2007b) Picobiliphytes: a marine picoplanktonic algal group with unknown affinities to other eukaryotes. *Science* **315**: 253–255.
- Not, F., Latasa, M., Scharek, R., Viprey, M., Karleskind, P., Balagué, V., et al. (2008) Protistan assemblages across the Indian Ocean, with a specific emphasis on the picoeukaryotes. *Deep Sea Res Part I Oceanogr Res Pap* **55**: 1456–1473.
- Novarino, G., Mills, D.K., and Hannah, F. (1997) Pelagic flagellate populations in the southern North Sea, 1988–89. I. Qualitative observations. *J Plankton Res* **19**: 1081–1109.
- Pauly, D., and Christensen, V. (1995) Primary production required to sustain global fisheries. *Nature* **374**: 255–257.
- Robinson, C., Poulton, A.J., Holligan, P.M., Baker, A.R., Forster, G., Gist, N., et al. (2006) The Atlantic Meridional Transect (AMT) Programme: a contextual view 1995–2005. *Deep Sea Res Part II Top Stud Oceanogr* **53**: 1485–1515.
- Rodríguez, F., Derelle, E., Guillou, L., Le Gall, F., Vaultot, D., and Moreau, H. (2005) Ecotype diversity in the marine picoeukaryote *Ostreococcus* (Chlorophyta, Prasinophyceae). *Environ Microbiol* **7**: 853–859.
- Romari, K., and Vaultot, D. (2004) Composition and temporal variability of picoeukaryote communities at a coastal site of the English Channel from 18S rDNA sequences. *Limnol Oceanogr* **49**: 784–798.
- Schattenhofer, M., Fuchs, B.M., Amann, R., Zubkov, M.V., Tarran, G.A., and Pernthaler, J. (2009) Latitudinal distribution of prokaryotic picoplankton populations in the Atlantic Ocean. *Environ Microbiol* **11**: 2078–2093.
- Shi, X.L., Marie, D., Jardillier, L., Scanlan, D.J., and Vaultot, D. (2009) Groups without cultured representatives dominate eukaryotic picophytoplankton in the Oligotrophic South East Pacific. *PLoS ONE* **4**: e7657.
- Tarran, G.A., Heywood, J.L., and Zubkov, M.V. (2006) Latitudinal changes in the standing stocks of nano- and picoeukaryotic phytoplankton in the Atlantic Ocean. *Deep Sea Res Part II Top Stud Oceanogr* **53**: 1516–1529.
- Thronsen, J. (1996) The planktonic marine flagellates. In *Identifying Marine Phytoplankton*. Tomas, C.R. (ed.). San Diego, CA, USA: Academic Press, pp. 591–730.
- Vaultot, D., Romari, K., and Not, F. (2002) Are autotrophs less diverse than heterotrophs in the marine picoplankton? *Trends Microbiol* **10**: 266–267.
- Vaultot, D., Eikrem, W., Viprey, M., and Moreau, H. (2008) The diversity of small eukaryotic phytoplankton ( $\leq 3 \mu\text{m}$ ) in marine ecosystems. *FEMS Microbiol Rev* **32**: 795–820.
- Viprey, M., Guillou, L., Ferréol, M., and Vaultot, D. (2008) Wide genetic diversity of picoplanktonic green algae (Chloroplastida) in the Mediterranean Sea uncovered by a phylum-biased PCR approach. *Environ Microbiol* **10**: 1804–1822.
- West, N.J., Schönhuber, W.A., Fuller, N.J., Amann, R.I., Rippka, R., Post, A.F., and Scanlan, D.J. (2001) Closely related *Prochlorococcus* genotypes show remarkably different depth distributions in two oceanic regions as revealed by in situ hybridization using 16S rRNA-targeted oligonucleotides. *Microbiology* **147**: 1731–1744.
- Worden, A.Z. (2006) Picoeukaryote diversity in coastal waters of the Pacific Ocean. *Aquat Microb Ecol* **43**: 165–175.
- Worden, A.Z., and Not, F. (2008) Ecology and diversity of picoeukaryotes. In *Microbial Ecology of the Oceans*. Kirchman, D.L. (ed.). New York, NY, USA: John Wiley & Sons, Inc, pp. 159–196.
- Worden, A.Z., Nolan, J.K., and Palenik, B. (2004) Assessing the dynamics and ecology of marine picophytoplankton: the importance of the eukaryotic component. *Limnol Oceanogr* **49**: 168–179.
- Yuan, J., Chen, M.-Y., Shao, P., Zhou, H., Chen, Y.-Q., and Qu, L.-H. (2004) Genetic diversity of small eukaryotes from the coastal waters of Nansha Islands in China. *FEMS Microbiol Lett* **240**: 163–170.
- Zubkov, M.V., and Burkill, P.H. (2006) Syringe pumped high speed flow cytometry of oceanic phytoplankton. *Cytometry A* **69A**: 1010–1019.
- Zubkov, M.V., and Tarran, G.A. (2008) High bacterivory by the smallest phytoplankton in the North Atlantic Ocean. *Nature* **455**: 224–227.
- Zubkov, M.V., Sleight, M.A., Tarran, G.A., Burkill, P.H., and Leakey, R.J.G. (1998) Picoplanktonic community structure on an Atlantic transect from 50°N to 50°S. *Deep Sea Res Part I Oceanogr Res Pap* **45**: 1339–1355.
- Zubkov, M.V., Sleight, M.A., Burkill, P.H., and Leakey, R.J.G. (2000) Picoplankton community structure on the Atlantic Meridional Transect: a comparison between seasons. *Prog Oceanogr* **45**: 369–386.
- Zwirgmaier, K., Heywood, J.L., Chamberlain, K., Woodward, E.M.S., Zubkov, M.V., and Scanlan, D.J. (2007) Basin-scale distribution patterns of picocyanobacterial lineages in the Atlantic Ocean. *Environ Microbiol* **9**: 1278–1290.

## Supporting information

Additional Supporting information may be found in the online version of this article:

**Fig. S1.** Chemical and physical parameters along the AMT15 cruise track. Contour plots indicate nutrient or pigment concentrations (nitrite, nitrate, phosphate, silicate, chlorophyll or dissolved oxygen) or physical measurements (temperature, salinity) plotted as a function of light intensity (% surface irradiance, y-axis) along the cruise track (latitude degrees north or south of the equator, x-axis). Black contour lines indicate the depth in metres, black dots represent sampling points. Redrawn from Zwirgmaier and colleagues (2007).

**Fig. S2.** Rarefaction curves for the nuclear 18S rRNA and plastid 16S rRNA gene clone libraries constructed along AMT15.

**Table S1.** Environmental parameters along AMT15 associated with the constructed plastid and nuclear clone libraries.

Please note: Wiley-Blackwell are not responsible for the content or functionality of any supporting materials supplied by the authors. Any queries (other than missing material) should be directed to the corresponding author for the article.